MASCOT - ASTEROID LANDER WITH INNOVATIVE MOBILITY MECHANISM

J. Reill, H.-J. Sedlmayr, P. Neugebauer, M. Maier, E. Krämer, and R. Lichtenheldt

DLR (German Aerospace Center), Robotics and Mechatronics Center, Münchener Str. 20, 82234 Wessling, Germany
E-mail: Josef.Reill@dlr.de

ABSTRACT

The Mobile Asteroid Surface Scout (MASCOT) is already on its way to the C-type asteroid 1999 JU3. On 3rd December 2014 at 05:22 CEST, a JAXA H IIA launch vehicle lifted off from the Tanegashima Space Center and the Hayabusa-II spacecraft together with its MASCOT lander began their journey through space. After a cruise of almost four years, Hayabusa-II with MASCOT will reach their target, where MASCOT will descend to the surface of the asteroid. An innovative hopping mechanism, developed at DLR's Robotics and Mechatronics Center (RMC), allows the lander to upright to nominal position and to relocate on asteroid surface by hopping. A big advantage of this movement principle is the independence of the surrounding environments like rocks or craters due to the fact that all moveable parts are inside the lander. The mobility concept was developed based on Multi-Body-System simulation and verified by a zero-g flight test campaign. This paper gives an overview of the mission, the challenges, the development process and the actual status of mobility subsystem. The first checkout after launch was conducted and detailed analysis shows nominal operation.

1. INTRODUCTION

In the time from 2004 to 2011 a two degree of freedom robotic arm was mounted on the outside of ISS at the Zvezda module. During this ROKVISS (robotics component verification on ISS) experiment the Robotics and Mechatronics Center (RMC) of DLR in Oberpfaffenhofen gained a lot of experience in robotic systems for space applications (see [1], [2] and [3]). The developed components were tested and investigated as the robotic arm was tele-manipulated with closed force feedback loop. When returned back to earth in 2011 the mechanical and electrical components could be analyzed as well. The robotic joints were optimized and formed to an advanced modular actuation unit for space applications. As there is the need for different motor sizes depending on application also a scaling method was developed. Due to the high torque output of permanent magnet synchronous motor topology very powerful and compact systems like for example the space qualifiable DEXHAND were built (see [4], [5] and [6]). The same technology is also used to build a rover locomotion sub system [7] or a robotic arm for space projects.
This paper presents results of drivetrain further development that led to the actuation unit for MASCOT project. The challenges were the space and mass restrictions on the one hand and to overcome the risk of cold welding during the long cruise phase of approximately four years. During the cruise phase multiple check outs will be performed. These check outs could be used to analyze the health of the overall mobility subsystem including the mechanical parts. The possible increase of friction will result in an increased motor current which is one of the parameters that is monitored during the active check out of the subsystem. Also redundant power electronics, adapted to the needs of Hayabusa-II mission is shown. Fig. 1 shows an artists impression of the mission with the Hayabusa-II spacecraft and the deployed MASCOT lander.

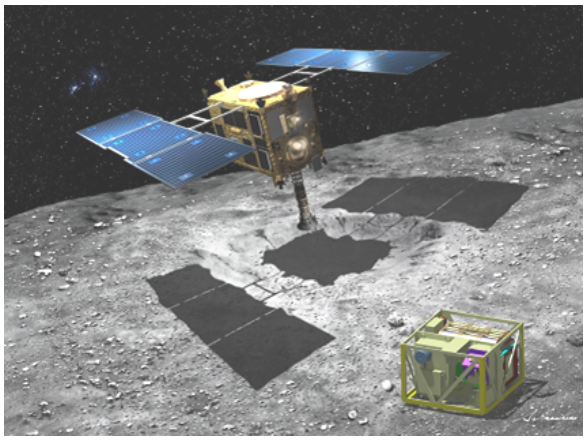

Figure 1. DLR artist's impression of the Hayabusa-II mission with MASCOT deployed.

The asteroid lander unit called MASCOT (Mobile Asteroid Surface Scout) is a 11 kg, cuboid shaped unit with the size of 300 mm x 300 mm x 200 mm. With camera, infrared radiometer, magnetometer and near infrared hyperspectral microscope there are four scientific experiments on board weighting in total 3 kg. As some instruments need nominal orientation for proper performance, GNC (guidance, navigation and control) sensors and a mobility mechanism for up righting and relocation on as-

teroid surface was required. For solving the mobility task additional challenges as compared to the ROKVISS experiment needed to be taken into account. Besides vacuum condition and thermal aspects the MASCOT mobility constraints were radiation stress of 10 kRad and increased risk of cold welding. On 3rd December 2014 the mission was launched at Tanegashima space center and will travel to the asteroid 1999 JU3 until July of 2018. During that long time almost no movement of the mechatronic hardware is planned. This leads to a high risk of cold welding within the bearings and gear unit.
The developed mechanics uses a small brushless DC motor with only 25 mm in diameter to accelerate and decelerate an eccentric arm. Because of resulting reactive force jerk is applied to the overall system and MASCOT can hop on asteroid surface. The trajectories are computed and optimized offline dependent on the specific asteroid parameters. For every orientation there are three trajectories with different intensity levels put in the MASCOT autonomy manager MAM. Once the lander is on asteroid surface the up righting and hopping is initiated autonomously.
All mobility electronics functionality is put on a single PCB, sized 95 mm x 105 mm in total for both redundancy paths. The system is designed for -55 up to 100°C storage and -40 up to 80°C operating temperature. Depending on the landing site on asteroid the temperature range varies very much. Furthermore the landing site cannot be chosen precisely. MASCOT will be separated from Hayabusa-II at an altitude of 100 m and will fall to the asteroid surface where it will have a first touchdown approximately 30 minutes later. Depending on asteroid surface parameters MASCOT will bounce several times on the surface changing its final landing position and orientation.
In the next sections mechanics as well as electronics and simulation of the hopping principle is presented. Furthermore details on the first checkout are shown.

2. MOBILITY SYSTEM OVERVIEW

In [8] and [9] the process of finding a solution for the scientific needs of MASCOT is shown. The final setup consists of a light weight carbon structure that houses the instruments as well as infrastructure. There are no solar cells on board. Therefore MASCOT is completely dependent on its battery that supplies the on board computer OBC, power control and distribution unit PCDU, antenna and all other subsystems and experiments for roughly 12 hours. Within that time MASCOT will gather scientific data at two or three different locations on asteroid surface and send it to the Hayabusa-II spacecraft. The mobility subsystem is put as far away as practicable from MASCOT's center of mass. This enables the system to tilt over from any side even with just one degree of freedom actuated. The engineering and integration issues of MASCOT are shown in [10] and [11] as the development of mobility subsystem is presented in [12].
The mobility subsystem is built redundant as much as possible. Due to space and mass limitations the motor with eccentric arm could not be realized redundant. Fig. 2 gives an overview of the system structure showing the redundant parts in green and the non-redundant parts in red. The mobility PCB is supplied by PCDU that provides 5 V

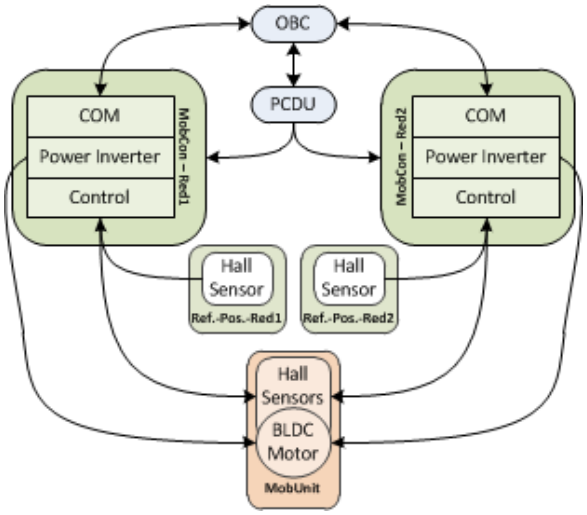

Figure 2. Block diagram of the mobility subsystem showing redundant (green) and non-redundant (red) components.

and 3V3 line for logic ICs and battery voltage as DC voltage for motor power inverter. Active redundancy path is chosen by switching on/off supply power (cold redundant principle). Communication with OBC is realized via RS-422. The demand for high reliability and high torque output at low mass and volume led to the solution with a brushless DC motor combined with Harmonic Drive gearing. In the following chapters more details are given on mechanics and electronics. Fig. 3 shows the flight model of controller PCB MobCon and motor without eccentric arm. The installation position of PCB and motor in MASCOT electronics box is just about the same as shown in the picture. The motor is inside and the eccentric arm is outside of the electronics box. The PCB is attached

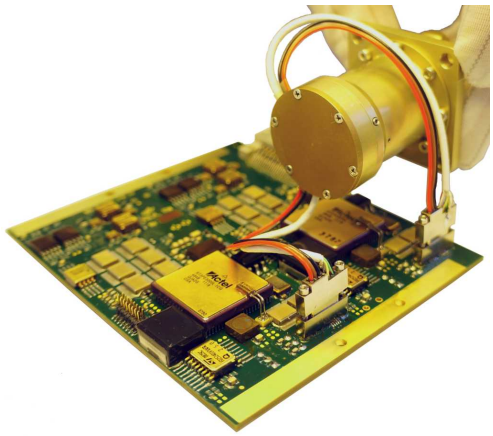

Figure 3. Photo image taken from the mobility flight model showing the PCB and estimated installation position of the motor.

to the electronics box with wedge locks and connected to a backplane that connects all PCBs from subsystems, experiments, PCDU and OBC.

3. DETAILS ON THE MECHANICS

Fig. 4 gives some details on the developed compact mechatronic system. Motor dimensions are cylindrical 25 mm x 10 mm. The number of mechanical components in the drive unit consisting of

- motor stator,
- motor rotor with permanent magnets,
- rotor bearing,
- Harmonic Drive wave generator,
- Harmonic Drive flex spline,
- Harmonic Drive circular spline and
- output bearing

is very low compared with solutions using brushed motors or multistage gearbox. Radiation hardened hall sensors are mounted inside the motor housing to get commutation information. Next to the motor there is the Harmonic Drive gearing consisting of circular spline (bright green), flex spline (green) and wave generator (dark blue). The eccentric arm (violet) is supported by an extra bearing (bright blue) and attached to the shaft by a screw (red) that also serves as a MLI foil standoff. Fig. 5 shows the

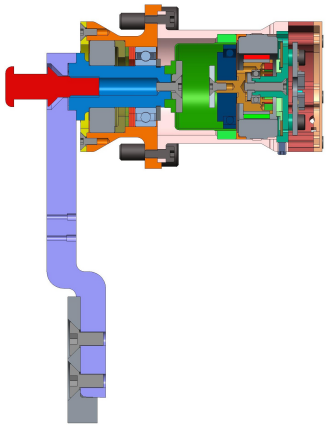

Figure 4. CAD sectional drawing of mobility unit (MobUnit) showing the compact fusion of Harmonic Drive gearing with brushless DC motor.

overall mobility unit (MobUnit). Since there is only a relative position measurement by use of motor hall sensors there is also a reference position sensor necessary. The motor flange is mounted to the electronics box as well as the reference position hall sensor (grey). There is a redundant hall sensor on this PCB and reference magnets on the eccentric arm. After performing a reference run the absolute position of the eccentric arm is known. The

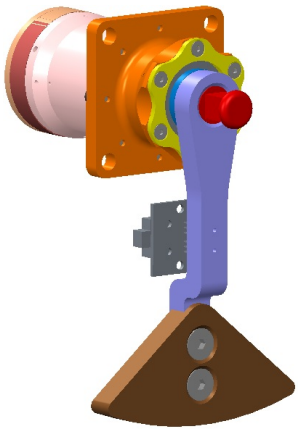

Figure 5. CAD image of motor and eccentric arm.

lubrication of the output shaft ball bearing is achieved by a combination of stainless steel rings, peek bearing cages and ceramic balls. This solution complies a non-metallic metallic combination that prevents cold welding. For the gearing bearing no hybrid ball-bearing could be found in the appropriate size. Therefore MoS2 lubrication was used there and on the gear teeth. Finally a dicronite DL-5 coating was applied to the harmonic drive wave generator bearing. It is of strong importance that mobility in MASCOT is no continuously running application. The mechanism is only activated for very short time and is at standstill for the rest of mission duration.

4. DETAILS ON THE ELECTRONICS

The mobility electronics needs to realize several functionality.

- communication with OBC
- collecting sensor data
- handle safety issues
- compute the absolute position of eccentric arm
- control of motor trajectory
- provide safety features

One of the central parts of mobility electronics is the power electronics of motor drive section. For a brushless DC motor (BLDC) motor, six power MOSFETs must be driven by the control unit. The interface between the mobility control unit (FPGA) and the power MOSFETs is realized by means of a high and low side gate driver. This gate driver is available as radiation tolerant part, but due to the space restrictions a Spin-In of an automotive BLDC motor controller and MOSFET driver was treated

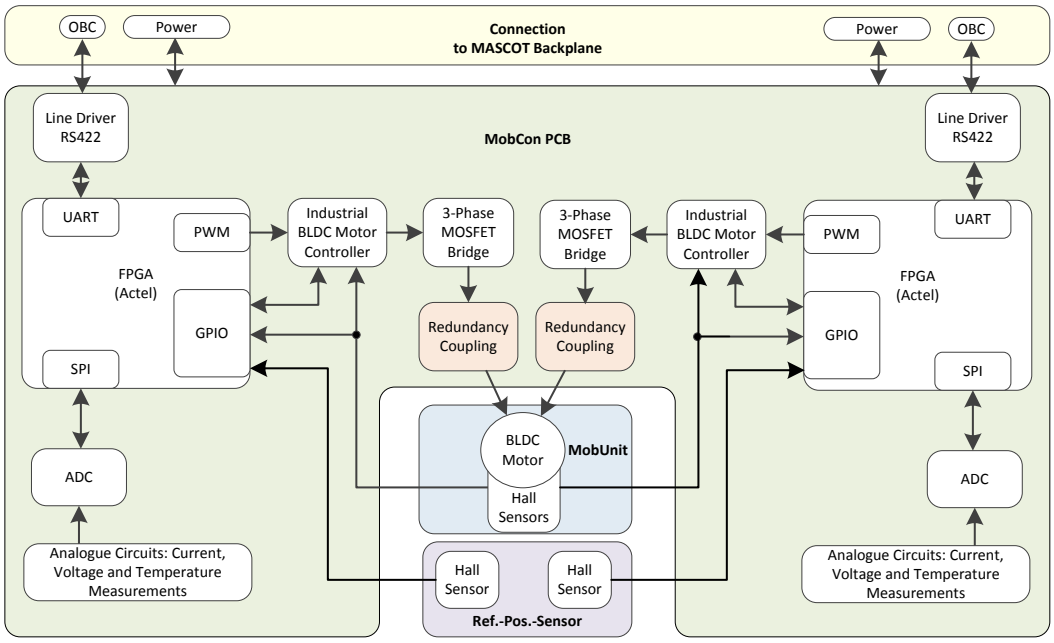

Figure 6. Detailed block diagram of the mobility subsystem with all interfaces.

as best way to meet the space and system requirements. For the MASCOT mission a total ionizing dose (TID) of 4.2 kRad (incl. margin) is expected within the electronics box. To provide additional margin, a minimum of 10 kRad was treated as criterion for the selection of the electronics. Of course, the used BLDC motor controller had to succeed several radiation tests, before it was used. These tests were performed at the Helmholtz Zentrum Berlin Wannsee, Germany [13] (TID and protons) and at the radiation effects facility in Jyvaskyla, Finland [14] (Heavy Ions). More details about the radiation tests and the detailed results are shown in [12].

Fig. 6 shows a block diagram of the mobility system whereby the mobility electronics is realized fully redundant. The FPGA computes a PWM signal depending on the acquired sensor data. This signal equals the desired phase voltage amplitude of the motor. The controller chip considers the motor hall signal pattern and activates the MOSFETs accordingly.

Driving a non redundant BLDC motor by redundant power inverter could be a bit tricky in case of a malfunction. Fig. 7 shows a simple redundancy coupling for one redundant half bridge which is connected to one non redundant motor winding. This coupling principle is working fine for a damaged MOSFET which is not responding to the gate control signal (permanently non conductive). But if one of the both low side MOSFETs T2 or T2' has a shot through, the whole drive electronics (both redundancy levels) is damaged, due to a short circuit in case of an regularly activated high side MOSFET T1 or T1'. Even if a redundant motor is coupled to a redundant drive electronics, it might be dangerous.

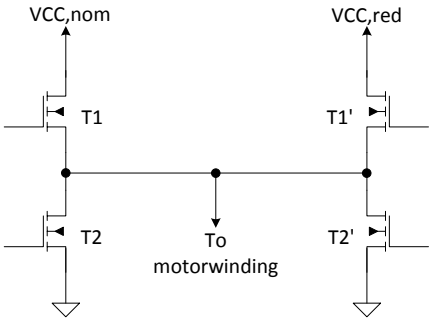

Figure 7. Schematic of simplified redundancy coupling.

The permanent magnets on the moving rotor cause flux alterations in the unused (redundant) motor phase and induce voltage. According to Eq. (1) [15] the induced voltage u is increasing with the number of windings N (per phase) and the motor speed. When there is a malfunction with one of the redundant MOSFET bridges a path for short current is possible. It is very important to prevent the current from flowing, otherwise the redundant winding would behave like an electro-magnetic brake. This additional load on the nominal motor leads to a slowdown of the intended movement or in case of a closed speed control loop, the running motor could be overloaded. If a redundant solution would have been possible for the mobility drive unit, an overload situation

were very unlikely due to the limited supply current. But in that case the movement would have been slowed down which prevents the MobUnit form initiating a movement of the MASCOT lander.

$$u = -N \cdot \frac{d\phi}{dt} \tag{1}$$

As described above, a decoupling network is necessary to design a fail save system, regardless whether you are running a full redundant or a partial redundant system. In Fig. 6 it is titled as „Redundancy Coupling“. Speaking simplified, the redundancy coupling is a switch which is added between the MOSFETs and the motor winding. Fig. 8 shows the principle of the added fail save redundancy coupling with the added switches RC and RC'. Regardless of the state of the low side MOSFETs T2 or

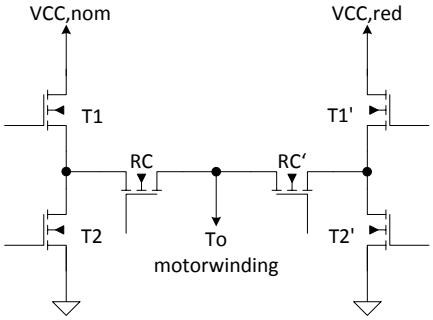

Figure 8. Schematic of fail save redundancy coupling.

T2', no unintentionally short circuit between the nominal and redundant side will occur due to the added switches. Of course, if one of the MOSFETs RC or RC' is not working properly (permanently non conductive), the associated side is blocked, or if one of both MOSFETs RC or RC' is permanently conductive, one will end up with the risks of the simplified redundancy coupling which is shown in Fig. 7.
Talking in terms of system availability these risks are easier to mitigate compared with the risks of the simplified redundancy coupling where one single error could damage the whole system.

5. MULTI BODY SIMULATION AND VERIFICATION

Multi Body Simulation (MBS) models Fig. 9 are used to analyze the motion behaviour of the mobility system, as well as MASCOT's interaction with the asteroid surface [9]. The models have been used in order to support the development of the mobility system throughout the mission preparation and to analyze the dynamic behaviour of the system. The main features of this model are:

- dynamics and kinematics of the bodies of MASCOT

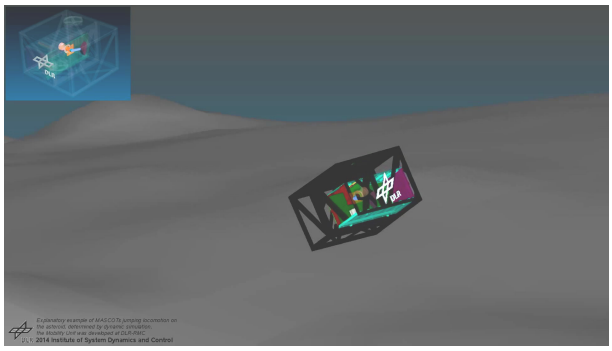

Figure 9. Animation output of MASCOT's MBS Model.

- contact dynamics including surface stick-slip friction between MASCOT and the asteroid surface modeled by PCM
- asteroid surface modeled to cover the extensions of 1999JU3
- soil parameters estimated from the current state of knowledge on 1999JU3
- height dependent gravity profile
- rigid or flexible modeling of MASCOT's outer CFRP-frame

Thereby the contact dynamics are modeled either as an elastic foundation surface by the Polygonal Contact Model (PCM) [16] implemented in SIMPACK or by the DLR Soil Contact Model (SCM) [17]. Applicable parameters for the ground contact can be found in [9]. Dependent on the desired level of detail, MASCOT's CFRP structure is modeled either as a simplified rigid body or as a flexible structure implemented into MBS by modal reduction of the CFRP structure's finite element model.
The models have been verified using both parabolic flight campaigns as well as high precision reaction force measurements (see Fig. 10) in order to determine the applicable frequency range the Multi Body model is able to reproduce. These comparisons have shown, that the model is able to reproduce the behaviour of the hardware in a frequency range of $f \in [3, 25]$ Hz. This range covers the region important for jumping. Higher frequency structural vibrations are not covered yet, but can be covered by incooperating further elastic effects of the lander structure by means of the flexible MBS model.
As the dependence of the desired jumping and up righting path of the MASCOT housing on the corresponding trajectory of the mobility unit arm is complex, suitable trajectories for all operational cases cannot be determined analytically. Even during parabolic flight campaigns low-gravity phases are not held sufficiently long in order to define the trajectories based on measurements. Thus MASCOT's Multi Body dynamics model is used to check the created trajectories. As 1999 JU3s surface parameters are only known with a limited accuracy, the usage of the elasto-plasctic PCM is considered sufficiently precise in order to compare different trajectories.

In order to systematically find suitable trajectories, the MBS models are applied to multi-criterial optimization using MOPS (Multi-Objective Parameter Synthesis) [18]. Using this approach combined with evolutionary strategies for global optimization enables to reliably find applicable trajectories in an automated process. In order to improve the convergence behaviour as well as the time efficiency, the parameters are optimized dependent on their mutual dependence. The main features of the optimization process are:

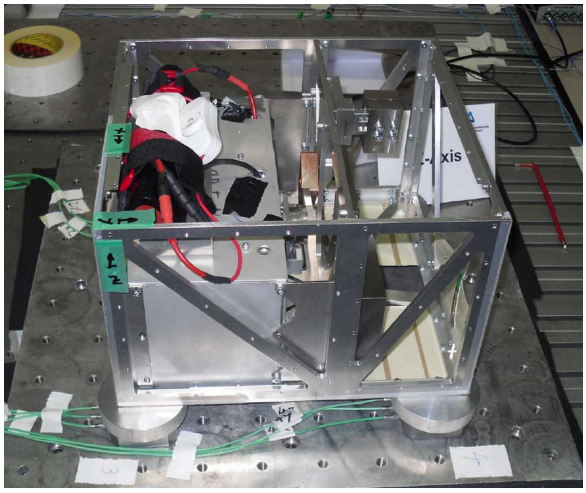

Figure 10. Measurement setup for the reaction forces in earth gravity.

- genetic algorithm to find global optima
- different scenarios and parameter cases
- input parameters as in real system

Thereby the objectives for the optimization are specifically defined for both, the up righting and the hopping scenario. When hopping in micro-gravity environments, keeping the upwards velocity safely below the escape speed is crucial in order to maintain operability of the system. Hence besides improving performance and reliability of the locomotion the approach enables to minimize and thus constrain MASCOT's upwards velocity to level safely contained below the escape speed.
The objectives used in the optimization of the hopping distance are used as listed below:

- jumping distance to first impact
- total jumping distance to the final equilibrium state, as a measure for uncertainty
- escape velocity as a binary objective working as upper boundary
- minimum jumping height and upwards velocity
- final housing box face and settling time after reaching equilibrium state

Evolutionary algorithms usually tend to need higher numbers of individuals and thus simulation iterations than deterministic approaches in order to find global optima. In this case the higher number of actual simulation runs can be used to further understand the micro-gravity interaction of landing gear and the asteroid surface.

6. HEALTH CHECK DATA

The first MASCOT health check during cruise phase of Hayabusa-II was conducted on 16th December 2014. In the applied health check sequence communication and system tests were conducted as well as subsystem tests. The mobility subsystem was investigated and the mechanics was moved at low speed to test for cold welding and friction issues.
The test was split into acquisition of housekeeping sensor data, searching the eccentric arm reference position and performing a complete trajectory maneuver with parameters causing only little jerk to the system. The maneuver itself is split into the commands "ready for movement" and "start movement". When mobility gets the "ready for movement" command the eccentric arm is moved to the trajectory start position. When this command is executed successfully the next command "start movement" initiates a complete trajectory. The eccentric arm is moved from start to end position with defined acceleration, deceleration and top speed. Both redundancy paths were tested and results were compared with flight model reference data taken right before launch.
The "search for reference position" was successfully completed even without moving the arm. The last test before launch was finished with the "search for reference position" command. There was no launch lock applied to the eccentric arm but still the vibrations and shocks during the launch did not move the arm at all. It was still at reference position. The electronics box temperature in the pre launch test was about 25°C and in the post launch during cruise phase it was -5°C . Due to operation it got warmed up a little. This difference of approximately 25 degrees is the main reason for an increase of friction.
With the successful detection of reference position the absolute position is known and the next command of the sequence was started. Fig. 11 shows the recorded data of the eccentric arm moving to start position. You can see the data of the flight model before (red signal plot) and after launch (blue signal plot) in direct comparison. The control strategy for that movement is implemented as hysteresis in open loop. PWM signal is proportional to motor voltage and is increased until a defined speed threshold is exceeded. When the motor is moving too fast the PWM signal is decreased again. Depending on the motor speed the PWM signal is also correlated with the motor current and with that it is correlated with the motor torque. The discrepancy of the given signal plots is due to the hysteresis that is implemented in the open loop threshold based principle. Since there is no closed loop speed controller activated, the different friction causes slower dynamics in the post launch signal.
The performance of the defined movement trajectory is

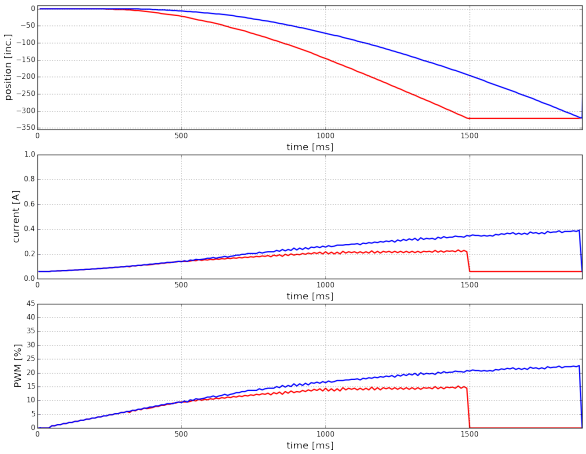

Figure 11. Go to start position maneuver, comparison of pre (red) and post (blue) launch data.

compared in Fig. 12. The "start movement" command

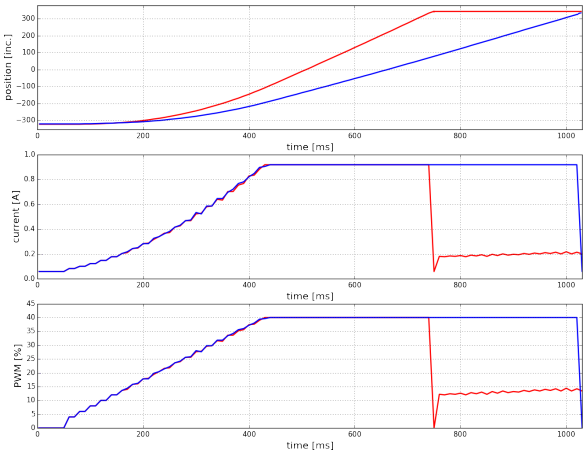

Figure 12. Start movement maneuver, comparison of data pre (red) and post (blue) launch.

sets the mobility controller in closed speed controller loop mode. Therefore the two signal plots should be identical as long as the movement parameters are set the same but for safety reasons the PWM signal was limited to 40%. Inside of Hayabusa-II careful movements are executed only. So again there is an explainable deviation of the two plots. The main purpose of the health check was not to perform an exact trajectory but to analyze friction behavior and to demonstrate the proper function of mechatronics.

7. CONCLUSION

The developed mobility system uses an innovative concept to relocate an asteroid lander. The reaction torque based principle enables a lander design that is independent on asteroid surface texture. Solutions that use mechanical actors like paddles that hit the ground typically suffer from the fact of small contact areas. The presented mechanism uses the whole system structure as a maximized push off area from the ground. Additionally it is much less affected by low contact forces due to microgravity like for example wheels are. One actor is sufficient to enable the system to relocate and upright. This helps to meet the strict requirements regarding mass and volume. Very high robustness is achieved by use of the realized hopping concept together with implementing the electronics completely redundant.
Despite the fact that the mechanism is very small and the risk of cold welding and increased friction is very high the first health check was conducted successfully. The health checks will be executed twice a year during the cruise phase and right before the decent to asteroid surface.

REFERENCES

[1] G. Hirzinger, K. Landzettel, D. Reintsema, C. Preusche, A. Albu-Schaeffer, B. Rebele, and M. Turk. ROKVISS robotics component verification on ISS. In *8th Int. Symposium on Artifical Intelligence, Robotics and Automation in Space - iSAIRAS*, Munich, Germany, 2005.

[2] A. Albu-Schaeffer, W. Bertleff, B. Rebele, B. Schaefer, K. Landzettel, and G. Hirzinger. ROKVISS robotics component verification on ISS current experimental results on parameter identification. In *International Conference on Robotics and Automation - ICRA*, Orlando, USA, May 2006.

[3] B. Schaefer, K. Landzettel, and G. and Hirzinger. ROKVISS: orbital testbed for tele-presence experiments, novel robotic components and dynamics models verification. In *8th Symposium on Advanced Space Technologies in Robotics and Automation (ASTRA)*, ESA/ESTEC, Noordwijk, Netherlands, November 2004.

[4] A. Wedler, M. Chalon, K. Landzettel, M. Goerner, E. Kraemer, G. Gruber, A. Beyer, H.-J. Sedlmayr, B. Willberg, W. Bertleff, J. Reill, M. Grebenstein, M. Schedl, A. Albu-Schaeffer, and G. Hirzinger. DLR's dynamic actuator modules for robotic space applications. In *41th Aerospace Mechanisms Symposium AMS*, Pasadena, USA, May 2012.

[5] A. Wedler, M. Chalon, A. Baumann, W. Bertleff, A. Beyer, R. Burger, J. Butterfass, M. Grebenstein, R. Gruber, F. Hacker, E. Kraemer, K. Landzettel, M. Maier, H.-J. Sedlmayr, N. Seitz, F. Wappler, B. Willberg, T. Wimboeck, F. Didot, and G. Hirzinger. DLR's space qualifiable multi-figered DEXHAND. In *11th Symposium on Advanced Space Technologies in Robotics and Automation (ASTRA)*, ESA/ESTEC, Noordwijk, Netherlands, April 2011.

[6] A. Wedler, A. Maier, J. Reill, C. Brand, H. Hirschmueller, M. Suppa, A. Beyer, and R. Haarmann. Pan/Tilt-Unit as a perception module for extra-terrestrial vehicle and landing systems. In

12th Symposium on Advanced Space Technologies in Robotics and Automation (ASTRA), ESA/ESTEC, Noordwijk, Netherlands, May 2013.

[7] Armin Wedler, Bernhard Rebele, Josef Reill, Michael Suppa, Heiko Hirschmüller, Christoph Brand, Martin Schuster, Bernhard Vodermayer, Heinrich Gmeiner, Annika Maier, Bertram Willberg, Kristin Bussmann, Fabian Wappler, and Matthias Hellerer. LRU - Lightweight Rover Unit. In *Proc. of the 13th Symposium on Advanced Space Technologies in Robotics and Automation (ASTRA)*, May 2015.

[8] C. Dietze, F. Herrmann, S. Kuß, C. Lange, M. Scharringhausen, L. Witte, T. van Zoest, and H. Yano. Landing and mobility concept for the small asteroid lander MASCOT on asteroid 1999 JU3. In *61st International Astronautical Congress IAC*, Prague, Czech Republic, September 2010.

[9] F. Herrmann, S. Kuß, and B. Schaefer. Mobility challanges and possible solutions for low-gravity planetary body exploration. In *11th Symposium on Advanced Space Technologies in Robotics and Automation (ASTRA)*, ESA/ESTEC, Noordwijk, Netherlands, April 2011.

[10] J. T. Grundmann, V. Baturkin, J. Biele, A. Bellion, E. Canalias, L. Celotti, F. Cordero, M. Deleuze, R. Findlay, S. Fredon, C. Grimm, J. Hendrikse, F. Herrmann, T.-M. Ho, E Jurado, C. Krause, R. Kroth, E. Ksenik, S. Kuß, M. Lange, C. Lange, M. Maier, L. Melac, O. Mierheim, P. Neugebauer, T. Okada, S. Reershemius, J. Reill, B. Schäfer, H.-J. Sedlmayr, K. Stohlmann, N. Termtanasombat, S. Ulamec, M. Wrasmann, T. Yoshimitsu, C. Ziach, and T. van Zoest. You've got 2 years, 6 months, 1 week and 48 hours! – the ongoing engineering adventure of mascot and its implications for planetary defence missions. In *Planetary Defense Conference*, Flagstaff, Arizona, USA, April 2013.

[11] T.-M. Ho, R. Findlay, C. Ziach, C. Krause, M. Lange, J. Reill, M. Deleuze, S. Ulamec, J. Biele, R. Jaumann, J. P. Bibring, K.-H. Glaßmeier, M. Grott, M. H. Kuninaka, M. Yoshikawa, T. Okada, T. Yoshimitsu, and the MASCOT Team (2014). MASCOT (Mobile Asteroid Surface Scout) - developing a landing platform with four instruments for the hayabusa-2 mission. In *45th Lunar Planetary Conference*, Houston, Texas, USA, March 2014.

[12] J. Reill, H.-J. Sedlmayr, S. Kuß, P. Neugebauer, M. Maier, A. Gibbesch, B. Schaefer, and A. Albu-Schaeffer. Development of a mobility drive unit for low gravity planetary body exploration. In *12th Symposium on Advanced Space Technologies in Robotics and Automation (ASTRA)*, ESA/ESTEC, Noordwijk, Netherlands, May 2013.

[13] Helmholtz Zentrum Berlin Wannsee. Cobalt-60 source. $http://www.helmholtz-berlin.de/angebote/tt-industrie/methoden/kobalt/index_de.html$, 2015.

[14] University of Jyvaskyla. Radiation effects facility - RADEF. $https://www.jyu.fi/fysiikka/en/research/accelerator/radef/facility$, 2015.

[15] H. Grafe, J. Loose, and H. Kuehn. *Grundlagen der Elektrotechnik, Band 1*. Dr. Alfred Huethig Verlag, Heidelberg, 1985.

[16] G. Hippmann. *Modellierung von Kontakten komplex geformter Körper in der Mehrkörperdynamik*. PhD thesis, Technischen Universität Wien, 2004.

[17] R. Krenn and G. Hirzinger. Scm – a soil contact model for multi-body system simulations. In *In 11th European Regional Conference of the International Society for Terrain-Vehicle Systems, Bremen*, 2009.

[18] H.-D. Joos, J. Bals, G. Looye, K. Schnepper, and A Varga. A multi-objective optimisation-based software environment for control systems design. In *IEEE International Conference on Control Applications and International Symposium on Computer Aided Control Systems Design, Glasgow, Scotland, UK, S. 7-14*, 2002.